

Construction and Performance of the BABAR-DIRC*

Jochen Schwiening^a (representing the BABAR-DIRC Collaboration)

GSI Helmholtzzentrum für Schwerionenforschung GmbH

Planckstr. 1, 64291 Darmstadt, Germany

E-mail: J.Schwiening@gsi.de

The new type of ring-imaging Cherenkov detector technology called DIRC (an acronym for **D**etection of **I**nternally **R**eflected **C**herenkov (**L**ight)) has been used successfully for hadronic particle identification in the *BABAR* experiment at the B Factory (PEP-II) located at the SLAC National Accelerator Laboratory. This paper describes the R&D for and the construction of the DIRC radiator bars and the performance of the DIRC during more than eight years of B Factory operation.

The BABAR-DIRC Collaboration

R. Andreassen,⁸ D. Arnaud,⁴ D. Aston,¹ N. van Bakel,¹ E. Ben-Haim,³ J. Benitez,¹ D. Bernard,⁵ D.N. Brown,⁶ J. Chauveau,³ C. Dallapiccola,¹⁰ M. Escalier,² L. Esteve,² G. Grosdidier,⁴ J. Kaminski,¹ A.-M. Lutz,⁴ G. Mancinelli,⁸ B.T. Meadows,⁸ A. Perez,³ B.N. Ratcliff,¹ E. Salvati,¹⁰ J. Schwiening,¹ J. Serrano,⁴ M.D. Sokoloff,⁸ S. Spanier,⁹ A. Stocchi,⁴ K. Suzuki,¹ Ch. Thiebaux,⁵ G. Vasseur,² J. Va'vra,¹ R.J. Wilson,⁷ B. Wogsland,⁹ G. Wormser,⁴ M. Zito.²

¹ SLAC National Accelerator Laboratory, Stanford, California 94309, USA.

² CEA, Irfu, SPP, Centre de Saclay, F-91191 Gif-sur-Yvette, France.

³ Laboratoire de Physique Nucléaire et de Hautes Energies, IN2P3/CN RS, Université Pierre et Marie Curie-Paris6, Université Denis Diderot-Paris7, F-75252 Paris, France.

⁴ Laboratoire de l'Accélérateur Linéaire, IN2P3/CNRS et Université Paris-Sud 11, Centre Scientifique d'Orsay, B. P. 34, F-91898 Orsay Cedex, France.

⁵ Laboratoire Leprince-Ringuet, CNRS/IN2P3, Ecole Polytechnique, F-91128 Palaiseau, France.

⁶ Lawrence Berkeley National Laboratory and University of California, Berkeley, California 94720, USA.

⁷ Colorado State University, Fort Collins, Colorado 80523, USA.

⁸ University of Cincinnati, Cincinnati, Ohio 45221, USA.

⁹ University of Tennessee, Knoxville, Tennessee 37996, USA.

¹⁰ University of Massachusetts, Amherst, Massachusetts 01003, USA.

1. Introduction

The Particle Identification (PID) system used in *BABAR* [1] between 1999 and 2008 was a new kind of ring-imaging Cherenkov detector called the DIRC [2] (the acronym DIRC stands for *D*etection of *I*nternally *R*eflected *C*herenkov light). It was designed to provide excellent π/K separation for all tracks from *B*-meson decays from the pion Cherenkov threshold up to 4.2 GeV/c. During more than 8 years of operation the DIRC has proven to be robust, stable, and easy to operate [3]. The PANDA experiment at FAIR [4] plans to build a barrel DIRC detector [5] which is in many ways similar to the *BABAR* DIRC. This paper will discuss topics of relevance to the PANDA DIRC such as design and fabrication issues of the *BABAR* DIRC system as well as the operational and physics performance. Note that space limitations prevent much of the descriptive material presented in the talk from being included in this write-up.

*Work supported by Department of Energy contract DE-AC02-76SF00515 (SLAC), DE-AC03-76SF00098 (LBNL), DE-AM03-76SF0010 (UCSB), and DE-FG03-93ER40788 (CSU); the National Science Foundation grant PHY-95-11999 (Cincinnati).

2. Design

The DIRC principle, design, construction, and performance are described in detail in Ref. [3]. Briefly, the DIRC uses 4.9 m long, rectangular bars made from synthetic fused silica as Cherenkov radiator and light guide. A charged particle with velocity v , traversing the fused silica radiator with index of refraction n (~ 1.473), generates a cone of Cherenkov photons of half-angle θ_C with respect to the particle direction, where $\cos\theta_C = 1/\beta n$ ($\beta = v/c$, $c =$ velocity of light). For particles with $\beta \approx 1$, some photons always lie within the total internal reflection limit, and are transported efficiently to either one or both ends of the bar, depending on the particle incident angle. Since the bar has a rectangular cross section and is made to optical precision, the magnitude of the Cherenkov angle is conserved during the reflection at the radiator surfaces. The photons are imaged via “pin-hole” focussing by expanding through a standoff region filled with 6000 litres of purified water onto an array of 10752 densely packed photomultiplier tubes placed at a distance of about 1.2 m from the bar end. Imaging in the *BABAR* DIRC occurs in three dimensions, by recording the location and the time at which a given PMT is hit. The expected single photon Cherenkov angle resolution is about 9 mrad, dominated by a geometric term that is due to the sizes of bars, PMTs and the expansion region, and a chromatic term from the photon production. The accuracy of the time measurement is limited by the intrinsic 1.5 ns transit time spread of the PMTs.

3. Development and Construction

The primary requirements in the selection of the raw material for the DIRC radiators were radiation hardness, attenuation length, small chromatic dispersion, and the ability to allow an excellent optical finish. A number of candidate materials, including acrylic plastic and several types of natural and synthetic fused silica, were considered and subjected to a series of tests, described in detail in reference [6]. Perhaps the most fundamental results were:

- Natural fused silica materials, when exposed to a radiation dose as low as 5-10 krad, suffer from serious radiation damage, resulting in substantial transmission losses in the blue and UV. All synthetic fused silica samples, however, were found to be sufficiently radiation hard for *BABAR*.
- Some synthetic fused silica materials, made in the form of ingots, show periodic optical inhomogeneities. This effect can be sufficiently large to make the DIRC inoperable.

Two synthetic materials made by TSL (called Spectrosil 2000 and Spectrosil B [7]) met or exceeded all requirements and were chosen as the material for the DIRC bars, wedges and windows.

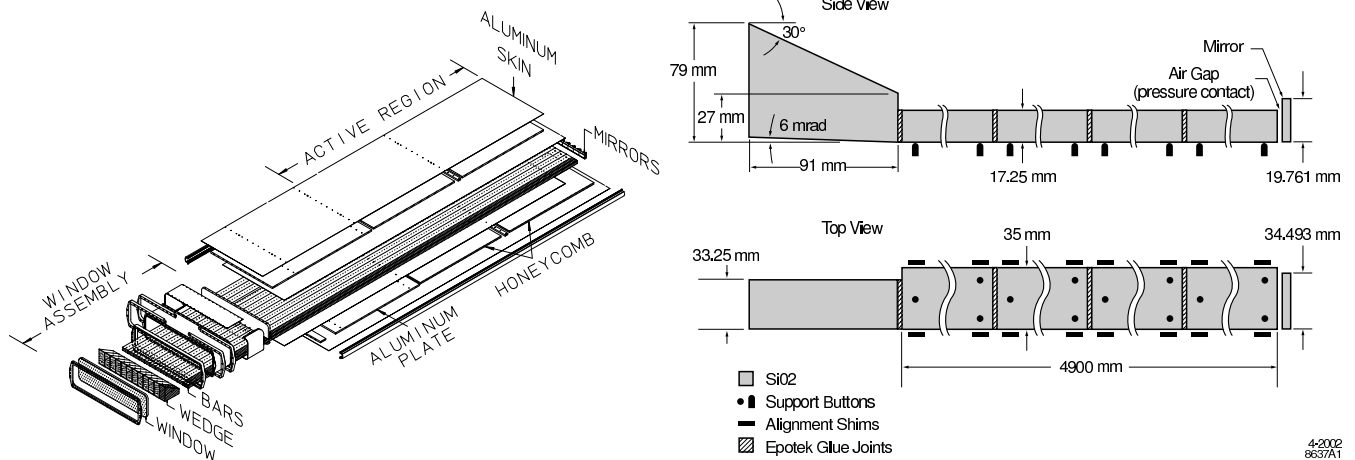


Figure 1: Schematic drawing of a bar box showing the active region, mirror end and window end (left) and of a DIRC radiator bar in side and top view (right).

The DIRC radiators took the form of long, thin bars with a nominal rectangular cross section (17.25 mm \times 35.0 mm). The individual 4.9 m-long units, referred to as “long-bars” during the production process, were each made up of four shorter 1.225 m-long pieces, referred to as “short-bars”, glued end-to-end. To each was attached a mirror on the forward end and a fused silica wedge on the backward (readout) end, shown schematically in Figure 1. The long-bars were placed 12 hermetically sealed containers, called bar boxes, each of which holds 12 radiator bars for a total of 144 bars.

The production tolerances for DIRC radiator bars were defined primarily by the physics performance goals of the DIRC system, specifically the Cherenkov angle resolution and the number of signal photons per track. The single photon Cherenkov angle resolution, for instance, is limited by such irreducible terms as size of PMTs, size of expansion region, and chromatic dispersion in the radiator material. Non-flatness and non-squareness of the bars cause the true Cherenkov angle to be smeared at every internal reflection. The magnitude of the resulting smearing term, and thus a limit of acceptable non-flatness and non-squareness, was determined from simulation.

The DIRC radiator bars were produced by Boeing [8]. The fabrication procedure was quite complex and was modified in a number of important ways as production proceeded and experience was gained. Though the basic geometrical requirements on surface figure are modest by optical standards, the required combination of elements, taken together, is very challenging to maintain in a production scale environment at modest cost. Some essential elements of good bars that provide particular challenges are (1) sharp edges, (2) excellent surface polish ($< 5 \text{ \AA}$ rms), and (3) good side-to-face orthogonality (a goal of $< 0.25 \text{ mr}$). In general terms, to obtain these basic elements in a production scale process, all large surfaces are ground on numerically controlled machines, lapped on a soft iron wheel, and then pitch polished on a 4 meter planetary pitch polisher. To avoid edge chips, all edges are processed either while protected by a neighboring bar, or with a glass plate glued onto the finished surface of the bar temporarily. Constant attention to detail in measurement and quality assurance (QA) is an essential element of the process. Full QA measurements were made throughout the process, and production units were reprocessed if they failed the specifications. Final QA measurement results are available for all the bars produced. The following description highlights some of the basic methodology of the process used for the majority of the bars, shown also schematically in Figure 2.

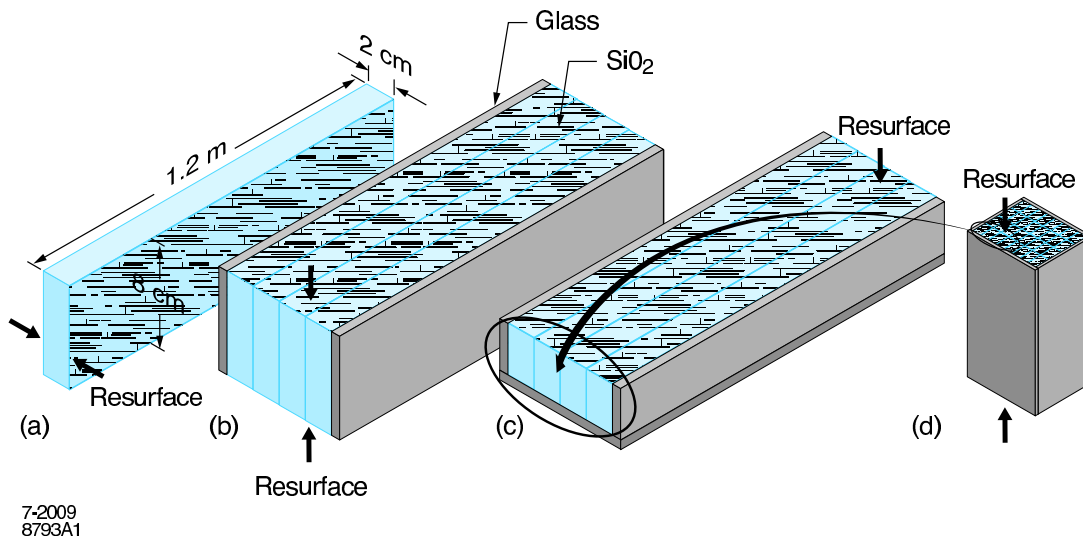


Figure 2: Schematic drawing of the primary stages of the radiator production process. (Dimensions are not to scale.)

The raw material was supplied by TSL in the form of ingots with approximate dimensions of 127 cm in length and 20 cm in diameter and an approximate weight of 90 kg. The ingots were sliced into 2-bar planks (units 1.95 cm \times 7.8 cm \times 124 cm) using a band saw for the long dimension and a chop saw for the ends [9]. The two large face surfaces (see Fig. 2a) of these planks then passed through the surfacing process (grind, lap, and polish) described

above. At the end of this process the planks had two high quality parallel faces with excellent surface polish ($< 5 \text{ \AA}$ rms). Four planks were then held by fixtures and glued together using a heat setting wax. The surfaces of the outer two planks were covered with glass planks for protection of the polished faces and edges. The two sides of these 8 bar units passed through the surfacing process again (see Fig. 2b). Then, they were sliced on a band saw, and the final side surface of each of the 4 bar sub-units produced was passed through the surfacing process (see Fig. 2c). Great care was taken to maintain the required face-to-face (side-to-side) parallelism and side-to-face orthogonality at each of these stages. At the end of this stage, all of the long surfaces had been completed. Finally, eight of the 4 bar units were glued into a 32 bar unit for the end processing (see Fig. 2d). The complete unit was ground to length on a custom grinder, and then placed upright on an over-arm custom built lapping-and-polishing machine to finish the ends to better than the required 2 nm rms surface finish. After disassembly, and final QA, the bars were carefully cleaned, and packed in specially designed units for shipping. A total of over 600 high quality fused silica bars were manufactured to our specifications (the DIRC contains 576).

4. Operational Issues

Soon after the DIRC was fully commissioned in late 1999, it achieved performance close to that expected from Monte Carlo simulation and ran efficiently and reliably until the end of B Factory operations in April 2008. The system has been robust and stable, and, indeed, served also as a background detector for PEP-II tuning. At the end of more than eight years of running, more than 98 % of PMTs and electronic channels were still operating with nominal performance. Details of the DIRC operational experience are described in Ref. [3]. This section describes two issues: the background in the DIRC and the PMT corrosion.

The background in the DIRC was dominated by low energy photons from the PEP-II machine hitting the water-filled standoff box. The time-to-digital converter (TDC) chip used originally in the DIRC data readout was designed such that a dead time of about 5% occurs at an input rate of 250kHz. Some care in machine tuning was required to stay under a limit of 250 kHz/tube. To monitor that rate, one PMT in each sector was read out via a scaler. In early 2000, at a peak luminosity value that corresponds to only one third of the design luminosity, the PMT rates reached a level that caused noticeable dead times. Due to those findings, lead shielding was installed for the DIRC. Since January 2001 an engineered, homogeneous lead shielding of 5cm to 8cm thickness covered the inside radius of the standoff box. This shielding kept the scaler rates well below a level of 300 kHz/tube even at luminosities that significantly exceeded the design luminosity.

During the shutdown that followed the 2001-2002 run, the TDCs were replaced with a faster version with deeper buffering capable of accepting a 2.5 MHz input rate with less than 5 % dead time. Ultimately, PEP-II reached a peak luminosity of $12.07 \times 10^{33} \text{ cm}^{-2}\text{sec}^{-1}$, four times the design value, without any dead time issues in the DIRC.

Some deterioration of the PMT front glass windows (made of B53 Borosilicate glass) that were immersed in the ultra-pure water of the standoff box has been observed since 2000, as shown in Figure 3. With water in the standoff box, these features were much less noticeable as water provides good optical coupling even to corroded glass. For most of the tubes, the observable effect was typically a slight cloudiness, but for about 50 tubes, it was much more pronounced and led to so-called *frosty* PMTs. Extensive R&D demonstrated that the effect was associated with a loss of sodium and boron from the surface of the glass. For most tubes, the leaching rate was a few microns per year, and was expected to be acceptable for the full projected ten year lifetime of the experiment. However, for the ~ 50 frosty tubes, the incorrect glass was used by the manufacturer. That glass did not contain zinc, making it much more susceptible to rapid leaching. It was thought that this leaching might eventually lead to either a loss of performance, or some risk of mechanical failure of the face plates for these tubes. However, until the end of *BABAR* operations in 2008 no such issues were observed.

Loss of photon detection efficiency can arise from this corrosion of PMT front glass windows as well as from possible deterioration of the water transparency or pollution of bar or window surfaces. Direct measurements of the number of Cherenkov photons observed in di-muon events as a function of time can be used to determine any degradation of the photon yield. An analysis, performed after about 5 years of running, using di-muon events from late 1999

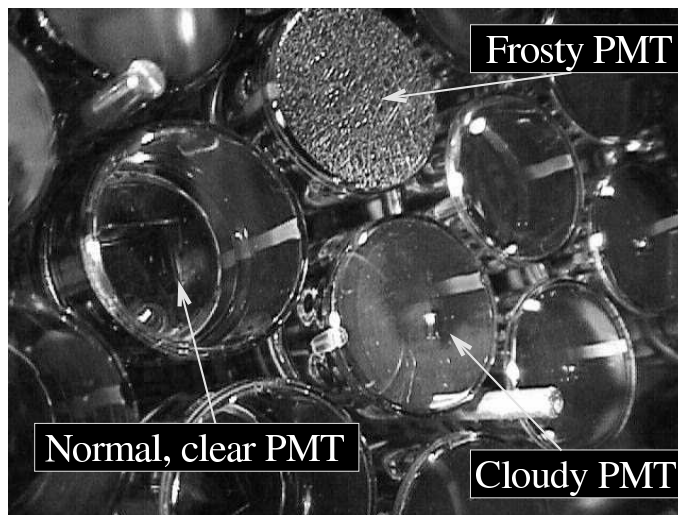


Figure 3: Example of PMT corrosion observed in October 1999, when the water was drained from the standoff box.

through July 2004, showed a photon loss rate of 1-2 %/year. There was no significant dependence of the loss rate on the radiator bar number, the position of track along the bar length, or the location of the Cherenkov ring in the PMT plane.

The reason for the loss in photon yield was not fully understood. The observed PMT glass corrosion may have contributed to the observed loss. While the number of frosty tubes is too small to cause a significant effect, the slight cloudiness affects most PMTs and is a possible source for part of the loss. R&D on photocathode aging, where DIRC PMT photocathodes were exposed to extremely large doses of UV light, ruled this mechanism out as explanation for the photon loss. Dynode aging, on the other hand, was one possible source as the DIRC PMTs have accumulated at least 30-40 Coulombs per anode in the first five years of operation. ADC calibrations in 2003 showed a loss of the PMT gain that was consistent with expected dynode aging. However, the lower PMT gain only accounted for about 30% of the observed loss in photon yield. Operationally, the PMT gain was recovered in 2003 by raising the high-voltage of the DIRC PMTs by an average of 43V. Nevertheless, even though the deterioration continued until April 2008 at the rate of 1-2%/year, the impact on the particle identification power of the DIRC was small. Even 10 years of photon loss at this level caused the the π/K separation at 3.5 GeV/c momentum to go from 3.5 standard deviations to 3.2 standard deviations.

5. Results

K/π separation is essential for the physics program of *BABAR*. The DIRC plays a central role in final state selection and B meson flavor tagging for CP measurements. This section provides an overview of the physics performance. A more detailed discussion of the use of DIRC in *BABAR* physics analyses can be found in Ref. [3].

In the absence of correlated errors, the resolution ($\sigma_{C,track}$) on the track Cherenkov angle should behave as:

$$\sigma_{C,track}^2 = \sigma_{C,\gamma}^2 / N_\gamma + \sigma_{track}^2 ,$$

where N_γ is the number of detected photoelectrons, $\sigma_{C,\gamma}$ is the single photon Cherenkov angle resolution and σ_{track} is the uncertainty of the track direction in the DIRC. Figure 4 shows the single photon angular resolution $\Delta\theta_{C,\gamma}$ obtained from di-muon events. There is a broad background of less than 10% relative height under the peak that originates mostly from track-associated sources, such as δ rays, reflections off the glue-fused silica boundaries, and combinatorial background. The width of the peak translates to a resolution of about 9.6 mrad, in good agreement with the expected value. The measured time resolution, shown in Figure 4, is 1.7 ns, close to the intrinsic 1.5 ns transit time spread of the PMTs.

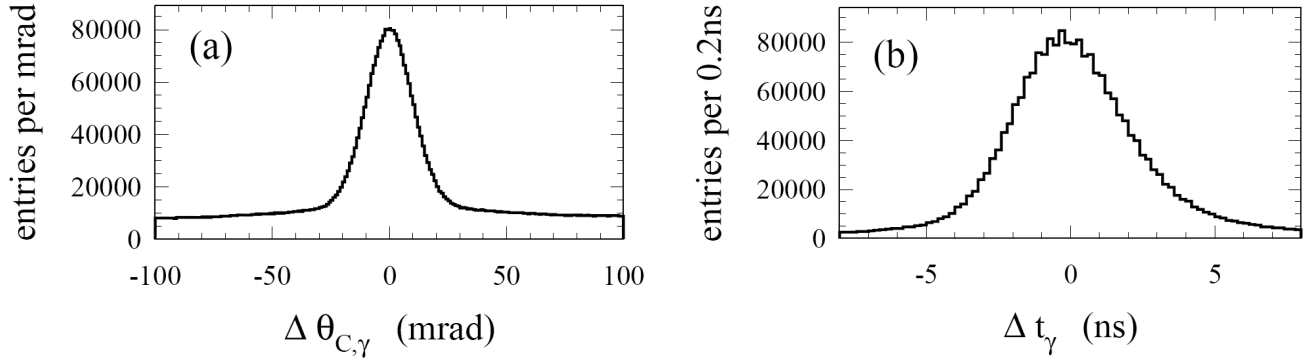


Figure 4: The difference between (a) the measured and expected Cherenkov angle for single photons, $\Delta\theta_{C,\gamma}$, and (b) the measured and expected photon arrival time, for single muons in $\mu^+\mu^-$ events.

The average value of N_γ , shown in Figure 5, varies between about a low of about 17 for tracks with small forward angles of incidence to nearly 60 for polar angles towards the forward and backward regions. The increase in the number of photons for tracks in the forward direction compensates for the reduced average separation in the Cherenkov angle for different particle hypotheses due to the increased track momenta in this region.

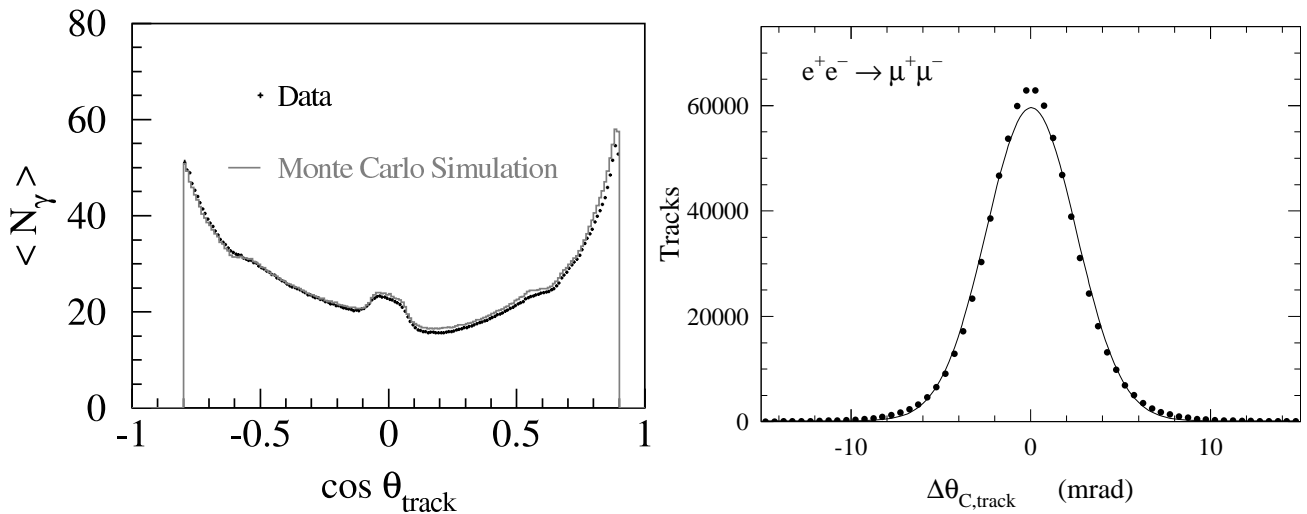


Figure 5: Number of detected photons versus track polar angle for reconstructed tracks in di-muon events compared to Monte Carlo simulation (left). The mean number of photons in the simulation has been tuned to match the data. Resolution of the reconstructed Cherenkov polar angle per track for di-muon events (right). The curve shows the result of a Gaussian fit with a resolution of 2.5 mr.

The Cherenkov angle resolution, $\sigma_{C,track}$, for tracks from di-muon events, $e^+e^- \rightarrow \mu^+\mu^-$, is shown in Figure 5. The width assuming a single Gaussian distribution is 2.5 mr. The resolution is 14 % larger than the design goal of 2.2 mr, which was estimated from the extensive study of a variety of prototypes, including a beam test.

The $D^{*+} \rightarrow \pi^+(D^0 \rightarrow K^-\pi^+)$ decay chain¹ is well suited to probe the pion and kaon identification capabilities of the DIRC. It is kinematically well constrained and the momentum spectrum of the charged pions and kaons covers the range accessible by B meson decay products in $BABAR$.

The pion-kaon separation power is defined as the difference of the mean Cherenkov angles for pions and kaons

¹Unless explicitly stated, charge conjugate decay modes are assumed throughout this section.

assuming a Gaussian-like distribution, divided by the measured track Cherenkov angle resolution. As shown in Figure 6, the separation between kaons and pions is about 4σ at 3 GeV/c declining to about 2.5σ at 4.2 GeV/c.

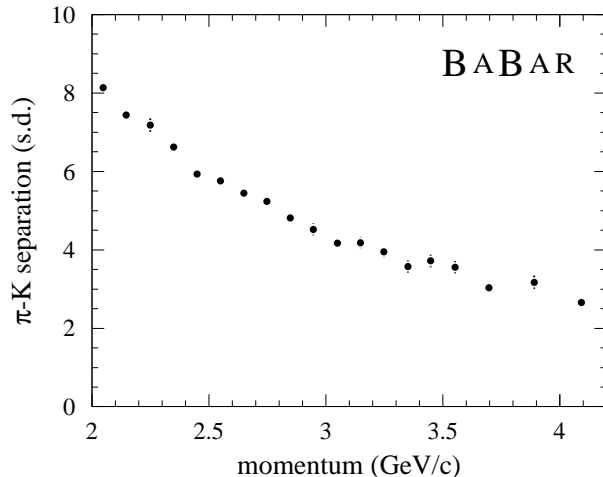


Figure 6: DIRC π -K separation versus track momentum measured in $D^0 \rightarrow K^- \pi^+$ decays selected kinematically from inclusive D^* production.

6. Summary

The DIRC is a novel ring-imaging Cherenkov detector that has proven to be very well-matched to the hadronic particle identification requirements of *BABAR*. The detector performance achieved was excellent and close to that predicted by the Monte Carlo simulations. The DIRC was robust, stable, and easy to operate and has played an important role in almost all *BABAR* physics publications. At the end of operations in 2008, after more than eight years of colliding beam data taking, more than 98 % of all PMTs and electronic channels were still operating with nominal performance.

References

- [1] B. Aubert et al., “The *BABAR* detector,” Nucl. Instrum. Methods Phys. Res., Sect. A **479** (2002) pp. 1-116.
- [2] B. N. Ratcliff, “The B factory detector for PEP-II: a status report,” SLAC-PUB-5946 (1992); B. N. Ratcliff, “The DIRC counter: a new type of particle identification device for B factories,” SLAC-PUB-6047 (1993); P. Coyle et al., “The DIRC counter: a new type of particle identification device for B factories,” Nucl. Instrum. Methods Phys. Res., Sect. A **343** (1994) pp. 292-299.
- [3] I. Adam et al., “The DIRC Particle Identification System for the *BABAR* Experiment,” Nucl. Instrum. Methods Phys. Res., Sect. A **538** (2005) pp. 281-357.
- [4] M. Kotulla et al., “Strong interaction studies with antiprotons. Letter of intent for PANDA,” Jan. 2004.
- [5] C. Schwarz et al., “The barrel DIRC of the PANDA experiment,” Nucl. Instrum. Methods Phys. Res., Sect. A **595** (2008) pp. 112-115.
- [6] J. Cohen-Tanugi, M. C. Convery, B. N. Ratcliff, X. Sarazin, J. Schwiening, J. Va’vra, “Optical Properties of the DIRC Fused Silica Cherenkov Radiator,” Nucl. Instrum. Methods Phys. Res., Sect. A **515** (2003) 680.
- [7] Spectrosil is a trademark of TSL Group PLC, Wallsend, Tyne on Wear, NE28 6DG, UK; Sold in the USA by Quartz Products Co., 160 W. Lee Street, Louisville, Kentucky 40201.

- [8] Boeing Optical Fabrication (now InSync, Inc.), 2511 C Broadbend Parkway NE, Albuquerque, New Mexico 87107.
- [9] Ideal Quartz Machining, 17990 Ideal Parkway, Manteca, California 95336.
- [10] Particle Data Group, K. Hagiwara et al., Phys.Rev. **D66**, 010001-1 (2002).